JOURNAL OF GEOPHYSICAL RESEARCH, VOL. 106, NO. B7, PAGES 13,435–13,442, JULY 10, 2001

Compacting and dilating shear bands in porous rock: Theoretical and experimental conditions

Pierre Bésuelle

Laboratoire de Géologie, Ecole Normale Supérieure, Paris, France

Abstract. The failure of rocks in the brittle regime is generally associated with the appearance of strain localization bands. For very porous rocks, three types of strain localization can be distinguished: extension bands, shear bands, and compaction bands. The first is associated with an extensional normal strain concentration inside the band; the second, with a shear strain concentration; and the third, with a compressive normal strain concentration. This paper shows the continuous transition between pure extension bands and pure compaction bands, via shear bands that evolve from dilating shear bands to compacting shear bands. By an extension to the analysis of *Rudnicki and Rice* [1975] (RR) on strain localization in pressure sensitive rocks, the prediction of the strain type inside bands at the onset of localization shows that inside shear bands, the shear strain can be associated with a volumetric dilatancy or compaction depending on the constitutive parameters of the material. The theoretical determination of the strain type is in accordance with recent observations of dilating and compacting shear bands in laboratory tests on porous sandstone specimens. A limit for the existence of a localized reduction of porosity within the band is expressed. A physical limit to the RR model is also proposed to insure continuity of the strain mechanism of localization with respect to the constitutive parameters.

1. Introduction

The phenomenon of porosity reduction inside strain localization bands has been observed in naturally deformed porous sandstone [*Antonellini et al.*, 1994; *Mollema and Antonellini*, 1996]. The deformation bands are thin and linear and often preferentially oriented with respect to the stress fields. These field observations show that strain localization bands are not necessarily associated with a dilatational strain but sometimes with a reduction of porosity. They suggest that such structures can locally reduce the permeability inside thin bands, which can have implications for petroleum reservoirs by changing the global permeability. Compacting shear bands have also been observed under laboratory conditions in a porous Vosges sandstone [*Bésuelle et al.*, 2000] and porous clays [*Tillard-Ngan et al.*, 1993; *Hicher and Wahyudi*, 1994]. *Olsson* [1999] has also discussed experimental observations of compaction bands. All of these results show that localized shear strain is often associated with a volumetric strain, which is dilating or compacting depending on the boundary conditions. Moreover, there is a continuous transition from dilating shear bands to compacting shear bands.

Paper number 2001JB900011.
0148-0227/01/2001JB900011$09.00

Rudnicki and Rice [1975] (hereinafter referred to as RR) proposed a model and a bifurcation analysis to predict the conditions for the onset of localized deformation in dilatant material. This work was extended by *Perrin and Leblond* [1993], who determined the limits for the possible existence of shear bands. *Olsson* [1999] and *Issen and Rudnicki* [2000] reinterpreted this result to analyze the existence of pure compaction bands in porous rocks. Pure compaction bands are bands that exhibit a normal compacting strain and a zero shear strain. Such bands have recently been recognized in the field [*Mollema and Antonellini*, 1996]. They can be explained in porous sandstone by the existence of a yield cap at high pressure. This yield cap is a compactive yield envelope with a negative pressure dependence [*Wong et al.*, 1997].

The aim of this paper is to extend the initial analysis of RR, by studying not only the conditions for the onset of localized bands that were already described, but also the predicted strain type inside the band at the onset of localization. This work shows the continuous evolution of the strain type with respect to the constitutive parameters between the pure extension bands and the pure compaction bands. It enables determination of the conditions for a compacting strain mechanism inside shear bands. These new theoretical results are well in accordance with experimental observations in laboratory tests.

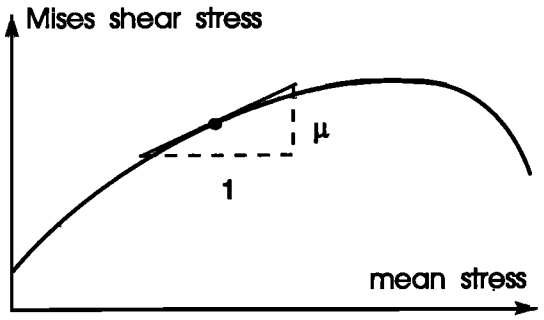

Figure 1. Schematic yield surface in the Mises shear stress versus mean stress plane. The slope of the curve (μ) decreases when mean stress increases.

2. Theoretical Conditions

2.1. Review of the Rudnicki and Rice Analysis

Rudnicki and Rice [1975] considered an elastoplastic constitutive law with a Drücker-Prager yield surface and a nonassociated flow rule to describe the response of brittle rocks. The yield surface delimits regions in stress space of elastic unloading and plastic loading. Such a yield surface is shown in Figure 1 in a plot of shear stress versus mean stress. The slope μ depends on the mean stress and is generally called a friction coefficient, except when it takes negative values. Figure 2a shows the relationship between the plastic volumetric strain and the plastic differential strain for a typical axisymmetric compression test where the slope of the curve is defined by using a dilatancy factor. Figure 2b shows axial stress as a function of plastic axial strain where the slope is defined by using a hardening modulus. The relation between the strain rate and the stress rate (compressive stress and strain are assumed to be negative) can be written as [*Rudnicki*, 1984]

$$D_{ij} = \frac{1}{2G}\left(\overset{\nabla}{\sigma}_{ij} - \frac{\nu}{1+\nu}\,\dot{\sigma}_{kk}\,\delta_{ij}\right) + \frac{1}{h}\,P_{ij}\,Q_{kl}\,\overset{\nabla}{\sigma}_{kl}\,, \quad (1)$$

where $D_{ij} = 1/2(v_{i,j} + v_{j,i})$ is the symmetric part of the velocity gradient tensor and $\overset{\nabla}{\sigma}$ and $\dot{\sigma}$ are the corotational Jaumann stress rate and the material derivative of stress, respectively. The first term is the elastic contribution with shear modulus G and Poisson coefficient ν; δ_{ij} is the Kronecker delta. The second term is the plastic contribution with the hardening modulus h, and the direction of the plastic strain rate is given by

$$P_{ij} = \sigma'_{ij}/2\bar{\tau} + (1/3)\,\beta\,\delta_{ij}\;; \quad (2)$$

where β is the dilatancy factor and the normal to the yield surface is given by

$$Q_{kl} = \sigma'_{kl}/2\bar{\tau} + (1/3)\,\mu\,\delta_{kl}\,, \quad (3)$$

and the Mises equivalent stress is

$$\bar{\tau} = \sqrt{\frac{1}{2}\,\sigma'_{ij}\sigma'_{ij}}\,, \quad (4)$$

where σ' is the deviatoric stress ($\sigma'_{ij} = \sigma_{ij} - 1/3\,\sigma_{kk}\delta_{ij}$). The constitutive relation can also be written as $\overset{\nabla}{\sigma}_{ij} = \mathcal{L}_{ijkl}\,D_{kl}$, with

$$\mathcal{L}_{ijkl} = G(\delta_{ik}\delta_{jl} + \delta_{il}\delta_{jk}) + \left(K - \frac{2}{3}G\right)\delta_{ij}\delta_{kl} - \frac{(G\sigma'_{ij}/\bar{\tau} + K\beta\delta_{ij})\,(G\sigma'_{kl}/\bar{\tau} + K\mu\delta_{kl})}{h + G + \mu\beta K}\,, \quad (5)$$

where K is the elastic bulk modulus.

RR studied the bifurcation conditions from a homogeneous stress and strain state to a band-localized strain state. They assumed a band normal to the x_2 coordinate axis and wrote the kinematic condition of the discontinuity of the strain rate as

$$\Delta D_{ij} = 1/2\,(g_i\delta_{j2} + g_j\delta_{i2})\,, \quad (6)$$

where ΔD_{ij} is an additional velocity gradient tensor inside the band with respect to the tensor outside the band and g_i is an arbitrary vector which varies only with position across the band. The equilibrium on the interfaces of the band is

$$\Delta\dot{\sigma}_{2j} = 0,\; j = 1,2,3\,, \quad (7)$$

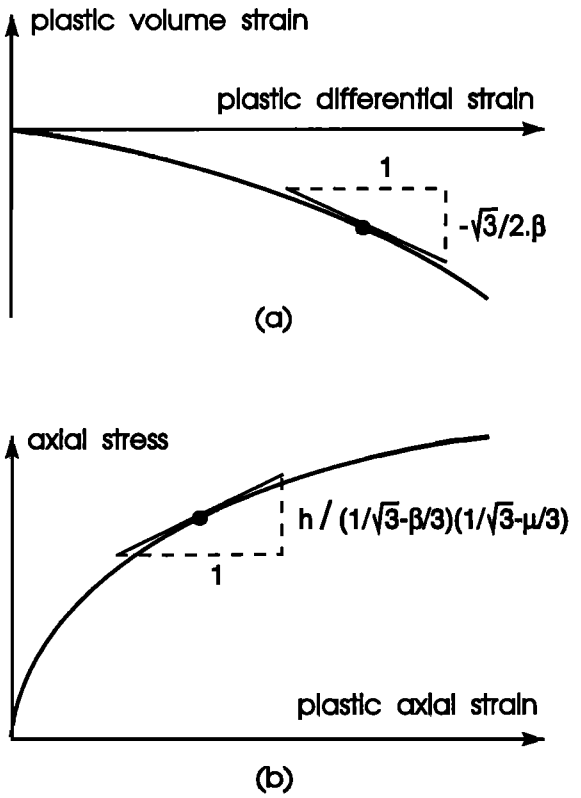

Figure 2. Schematic of a typical specimen response in an axisymmetric compression test. (a) Slope of the plastic volume strain versus the plastic differential strain using a dilatancy factor β. (b) Evolution of the axial stress with respect to the plastic axial strain using a hardening modulus h.

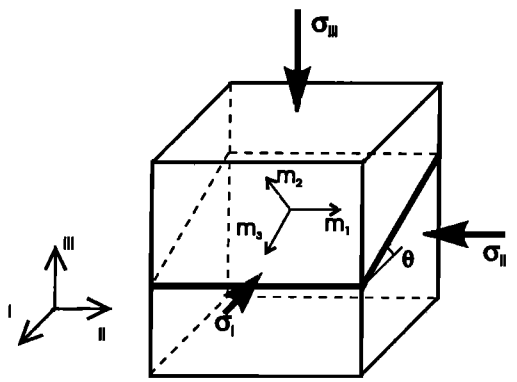

Figure 3. Definition of the local Cartesian system $m_1m_2m_3$, with respect to the principal stress directions $(\sigma_I, \sigma_{II}, \sigma_{III})$; θ is the angle between the band (the thicker line) and the σ_I direction.

where $\Delta\dot{\sigma}_{ij}$ is the difference of the stress rate tensor inside and outside the band. By considering (5)-(7), and approximating the Jaumann stress rate tensor to the material derivative of the stress tensor, the condition for the possible existence of a planar localization (i.e., the existence of a solution with $\mathbf{g} \neq 0$) is

$$\det(\mathcal{L}_{2jk2}) = 0\,; \tag{8}$$

from expression (5), the bifurcation condition (8) leads to the hardening modulus

$$\frac{h}{G} = \frac{(\sigma'_{22} + \beta K/G\bar{\tau})(\sigma'_{22} + \mu K/G\bar{\tau})}{(4/3 + K/G)\bar{\tau}^2} + \frac{{\sigma'_{21}}^2 + {\sigma'_{23}}^2}{\bar{\tau}^2} - 1 - \mu\beta K/G\,. \tag{9}$$

Rudnicki and Rice [1975] considered that the critical onset of bifurcation corresponds to the case of a maximum modulus h and searched the conditions on the Cartesian system orientation, where stress state was initially expressed, in comparison with the principal stress directions. The principal stresses are defined as $\sigma_I > \sigma_{II} > \sigma_{III}$ and the normalized deviatoric stresses are expressed by

$$\begin{aligned} N &= \sigma'_{II}/\bar{\tau} \\ N_I &= \sigma'_I/\bar{\tau} = -\tfrac{1}{2}N + \tfrac{1}{2}\sqrt{4 - 3N^2} \\ N_{III} &= \sigma'_{III}/\bar{\tau} = -\tfrac{1}{2}N - \tfrac{1}{2}\sqrt{4 - 3N^2}\,. \end{aligned} \tag{10}$$

The axisymmetric compression stress state $\sigma_I = \sigma_{II} > \sigma_{III}$ is defined by $N = N_I = 1/\sqrt{3}$, and the axisymmetric extension stress state $\sigma_I > \sigma_{II} = \sigma_{III}$ is defined by $N = N_{III} = -1/\sqrt{3}$; n_I, n_{II}, n_{III} are the projections of the unit normal to the band (the x_2 coordinate axis) on the three principal stress directions.

Perrin and Leblond [1993] showed in an elegant analysis that $n_{II} = 0$, $n_I \neq 0$, and $n_{III} \neq 0$ (i.e., the band is parallel to the intermediate principal stress direction) only in the following range of $(\beta + \mu)$:

$$(1 - 2\nu)N - \sqrt{4 - 3N^2} \leq \tfrac{2}{3}(1 + \nu)(\beta + \mu) \leq (1 - 2\nu)N + \sqrt{4 - 3N^2}\,. \tag{11}$$

It follows that one can write $n_I = \sin(\theta), n_{III} = \cos(\theta)$, where θ is the angle between the normal to the band and the σ_{III} direction. Expression (9) is maximized when

$$\tan^2(\theta) = (\xi - N_{III})/(N_I - \xi)\,, \tag{12}$$

where $\xi = (1 + \nu)(\beta + \mu)/3 - N(1 - \nu)$, which gives the critical hardening modulus

$$\frac{h_c}{G} = \frac{1 + \nu}{9(1 - \nu)}(\beta - \mu)^2 - \frac{1 + \nu}{2}\left(N + \frac{\beta + \mu}{3}\right)^2\,; \tag{13}$$

otherwise, outside the range of equation (11) [*Issen and Rudnicki*, 2000],

$$\frac{h_c}{G} = \frac{1 + \nu}{9(1 - \nu)}(\beta - \mu)^2 - \frac{1 + \nu}{1 - \nu}\left(\frac{1}{2}N_\zeta - \frac{\beta + \mu}{3}\right)^2 - \left(1 - \frac{3}{4}N_\zeta^2\right)\,, \tag{14}$$

with $\zeta = \mathrm{I}$ if the upper inequality of (11) is violated and $\zeta = \mathrm{III}$ if the lower inequality is violated.

The condition where $\zeta = \mathrm{III}$ corresponds to $n_I = n_{II} = 0$ and is possible if $(\beta + \mu)$ can be negative, which is realistic for porous rock due to a yield cap [*Olsson*, 1999; *Issen and Rudnicki*, 2000; *Wong et al.*, 1997] (see also the discussion in appendix I of RR's paper). This case corresponds to a band perpendicular to the axis of compression in an axisymmetric compression test and is discussed by *Olsson* [1999] and *Issen and Rudnicki* [2000] which they termed compaction bands. Extension bands are predicted for the case where $\zeta = \mathrm{I}$ and correspond to $n_{II} = n_{III} = 0$, i.e., a band parallel to the most compressive stress.

All these previous studies concentrated on the condition for localization by predicting the onset of localization (giving the critical hardening modulus h_c) and the orientation of the band with respect to the principal stress directions (the angle θ). The following section proposes an analysis of the strain inside the incipient localization band to determine the ratio between the volumic strain and the shear strain. My goal is to specify the type of strain that exists inside the band, which can be dilating, isovolumetrically shearing, or compacting.

2.2. Shear Strain and Volumetric Strain at the Onset of Localization

I examine the mechanism of localization, i.e., the expression for the discontinuity of the strain rate at the onset of localization. From the principal stress directions, the orientation of the band is defined by the angle θ. In any reference frame $Om_1m_2m_3$, where the second direction Om_2 is perpendicular to the band, the bifurcation condition (8) is met. For simplification, one can choose to take the first coordinate axis Om_1 to be equal to the second principal stress σ_{II} direction (Figure 3), which has no influence on the final result. The unit vectors of $Om_1m_2m_3$ are expressed in the principal stress

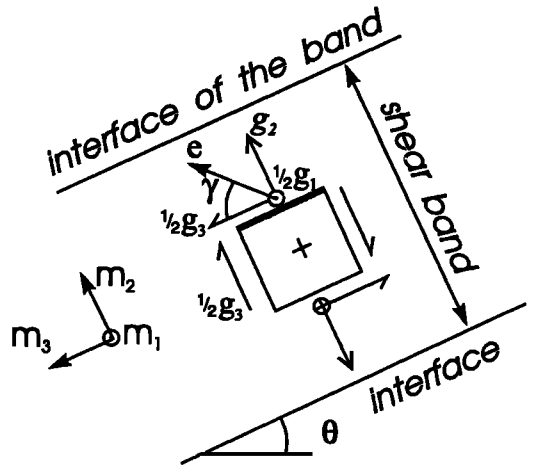

Figure 4. Strain rate inside the band expressed by the condition of discontinuity superimposed over the homogeneous strain rate. Vector **e** is the additional strain vector on a surface parallel to the interface of the band; γ is a band dilatancy angle.

directions reference system by $m_1 = (0,1,0)$; $m_2 = (\sin(\theta), 0, \cos(\theta))$; $m_3 = (\cos(\theta), 0, -\sin(\theta))$. In the $Om_1m_2m_3$ reference frame, the discontinuity of the strain rate (Figure 4) is expressed by

$$\Delta D_{ij} = \begin{pmatrix} 0 & \frac{1}{2}g_1 & 0 \\ \frac{1}{2}g_1 & g_2 & \frac{1}{2}g_3 \\ 0 & \frac{1}{2}g_3 & 0 \end{pmatrix} . \tag{15}$$

The terms g_1 and g_3 account for the shear strain inside the band, whereas g_2 accounts for the volumetric strain (g_2 is positive for dilatancy and negative for compaction). The nonsymmetric constitutive tensor $\mathcal{N}_{ij} = \mathcal{L}_{2i\,j2}$ is expressed by

$$\begin{aligned} \mathcal{N}_{ij} \;=\; & G(\delta_{i2}\delta_{j2} + \delta_{ij}) + (K - \tfrac{2}{3}G)\,\delta_{i2}\delta_{j2} \\ & - \frac{(G\sigma'_{i2}/\bar{\tau} + K\beta\delta_{i2})\,(G\sigma'_{j2}/\bar{\tau} + K\mu\delta_{j2})}{h + G + K\mu\beta} . \end{aligned} \tag{16}$$

The deviatoric stress in the $Om_1m_2m_3$ reference system is expressed from the principal deviatoric stresses by

$$\begin{aligned} \sigma'_{22} &= \tfrac{1}{2}(\sigma'_{\rm I} + \sigma'_{\rm III}) - \tfrac{1}{2}(\sigma'_{\rm I} - \sigma'_{\rm III})\cos(2\theta) \\ \sigma'_{12} &= 0 \\ \sigma'_{32} &= \tfrac{1}{2}(\sigma'_{\rm I} - \sigma'_{\rm III})\sin(2\theta) . \end{aligned} \tag{17}$$

By combining (16) and (17), the tensor $\mathcal{N}$ is reduced to the expression

$$\mathcal{N}_{ij} = \begin{bmatrix} G & 0 & 0 \\ 0 & \mathcal{N}_{22} & \mathcal{N}_{23} \\ 0 & \mathcal{N}_{32} & \mathcal{N}_{33} \end{bmatrix} , \tag{18}$$

where

$$\begin{aligned} \mathcal{N}_{22} &= 2G\tfrac{1-\nu}{1-2\nu} - \tfrac{G^2}{4(h_c+G+\mu\beta K)} \\ &\cdot \left[N_{\rm I} + N_{\rm III} - (N_{\rm I} - N_{\rm III})\cos(2\theta) + \tfrac{4}{3}\beta\tfrac{1+\nu}{1-2\nu}\right] \\ &\cdot \left[N_{\rm I} + N_{\rm III} - (N_{\rm I} - N_{\rm III})\cos(2\theta) + \tfrac{4}{3}\mu\tfrac{1+\nu}{1-2\nu}\right] \end{aligned} \tag{19a}$$

$$\begin{aligned} \mathcal{N}_{23} &= -\tfrac{G^2}{4(h_c+G+\mu\beta K)}(N_{\rm I} - N_{\rm III})\sin(2\theta) \\ &\cdot \left[N_{\rm I} + N_{\rm III} - (N_{\rm I} - N_{\rm III})\cos(2\theta) + \tfrac{4}{3}\beta\tfrac{1+\nu}{1-2\nu}\right] \end{aligned} \tag{19b}$$

$$\begin{aligned} \mathcal{N}_{32} &= -\tfrac{G^2}{4(h_c+G+\mu\beta K)}(N_{\rm I} - N_{\rm III})\sin(2\theta) \\ &\cdot \left[N_{\rm I} + N_{\rm III} - (N_{\rm I} - N_{\rm III})\cos(2\theta) + \tfrac{4}{3}\mu\tfrac{1+\nu}{1-2\nu}\right] \end{aligned} \tag{19c}$$

$$\mathcal{N}_{33} = G - \tfrac{G^2}{4(h_c+G+\mu\beta K)}(N_{\rm I} - N_{\rm III})^2\sin^2(2\theta) . \tag{19d}$$

The equilibrium equation (7) at the interface of the band is expressed by

$$\mathcal{N}_{ij}\, g_j = 0,\ i = 1,2,3 . \tag{20}$$

The first relation of (20) leads to $g_1 = 0$, which shows that the discontinuity of the strain state is a plane strain state in the plane determined by the major and minor principal stress directions. This means, if one considers an axisymmetric test, for example, that the strain becomes nonaxisymmetric at the onset of localization.

The second and third equations of (20) are equivalent since $\det(\mathcal{N}) = 0$. Consider now that **e** is the additional strain vector on a surface inside the band parallel to the interface of the band, i.e., $e_i = \Delta D_{i2}$ (Figure 4), and γ is the angle between the m_3 direction and **e**. The angle γ is defined by

$$\tan(\gamma) = -2\mathcal{N}_{23}/\mathcal{N}_{22} = -2\mathcal{N}_{33}/\mathcal{N}_{32} . \tag{21}$$

The component g_3 is chosen to be positive. If $\pi/2 > \gamma > 0$, then the shear strain is associated with a volumetric dilatancy, and if $-\pi/2 < \gamma < 0$, a volumetric compaction. The angle $\gamma = 0$ corresponds to a pure shear case with no dilation or compression; γ can be called the band dilatancy angle.

For low values of μ and β, the condition $\tan(\gamma) = \pi/2$ corresponds to the upper limit of (11) (i.e., $\theta = \pi/2$), while $\tan(\gamma) = -\pi/2$ corresponds to the lower limit (i.e., $\theta = 0$). The shear component of the strain discontinuity inside the band is zero when the band is parallel to the major or minor principal stress direction. This means that there is a continuous variation of the nature of the strain inside the band of localization, between the so-called shear bands and the pure extension or compaction bands. The condition $\tan(\gamma) = 0$ corresponds physically to a pure shear band, without volumetric strain. This condition is expressed by

$$3(1-2\nu)(1-\nu)N = (1+\nu)\left[(1-2\nu)(\beta+\mu) + 2\beta\right] . \tag{22}$$

The variation of γ is continuous with respect to μ and β (Figure 5a) for low values of μ and β. One can distinguish two zones in the plane (μ, β) which are called compacting shear bands and dilating shear bands, delimited by (22). Figure 5b shows the continuous evolution of the band orientation angle θ with respect to μ and β. The different domains (pure compaction bands, compacting shear bands, dilating shear bands, and pure extension bands) are also represented in Figure 6. The limit between the pure compaction band and the shear band and the limit between the pure extension band

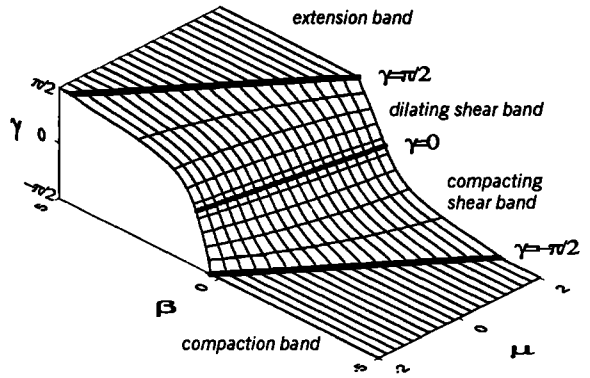

(a)

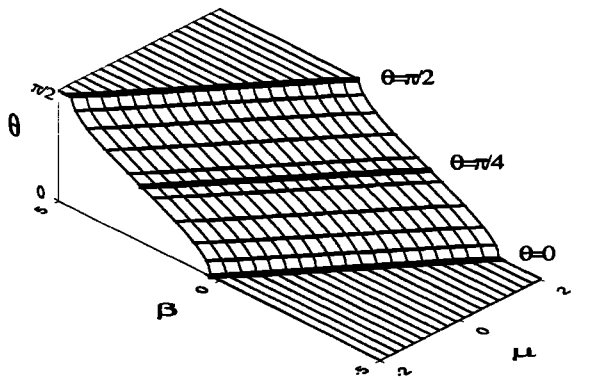

(b)

Figure 5. Evolution of (a) the band dilatancy angle γ and (b) the band orientation angle θ with respect to β and μ, for an axisymmetric compression stress state (i.e., $N = 1/\sqrt{3}$) and $\nu = 0.2$.

and the shear band are parallel and correspond to the values of $\theta = 0, \pi/2$ and $\gamma = -\pi/2, \pi/2$. Inside the area of shear band, the isovalue curves of θ are not parallel to the isocurves of γ, and one can have a pure shear band with an orientation θ lower or higher than $\pi/4$. For an associated plastic model (i.e., $\beta = \mu$), the conditions $\gamma = 0$ and $\theta = \pi/4$ are equivalent and can be written

$$\mu = \frac{3(1-2\nu)}{4(1+\nu)} N \,. \tag{23}$$

Nevertheless, for nonassociated models, the condition $\tan(\gamma) = 0$ can correspond to the limits of (11), for higher positive values or lower negative values of μ. In this condition, the vector $\mathbf{g}$ is undetermined. These limit values of μ and β are expressed by

$$\begin{aligned} \tfrac{4}{3}(1+\nu)\mu &= (1-2\nu)N \pm (3-2\nu)\sqrt{4-3N^2} \\ \tfrac{4}{3}(1+\nu)\beta &= (1-2\nu)N \mp (1-2\nu)\sqrt{4-3N^2} \,. \end{aligned} \tag{24}$$

Outside these values of μ, there is a discontinuity of the angle γ with respect to β at the limits of (11). This theoretical discontinuity of the strain mechanism is physically improbable and is considered to be a limitation of the RR formulation. However, for the range of different stress states (i.e., $-1/\sqrt{3} < N < 1/\sqrt{3}$) and $\nu = 0.2$, μ must be between -2.598 and 2.598 to assure continuity of γ. These values for μ are well within the estimated experimental range.

3. Comparison With Experimental Results

Experimental evidence of compacting shear bands in a porous Vosges sandstone (porosity of about 22%) has been obtained in an axisymmetric triaxial cell [*Bésuelle et al.*, 2000; *Bésuelle*, 1999]. The sandstone is a pink quartz sandstone (quartz, 93%) with a few percent of feldspar and white mica. The mean grain size is about 0.3 mm, and the diameter and the height of the specimens are 40 and 80 mm, respectively. Several axisymmetric compression tests (the compressive axial stress is higher than the compressive lateral stress) and axisymmetric extension tests (the compressive lateral stress is higher than the axial stress which can be compressive or extensive) have been performed from 0 to 60 MPa confining pressure with an axial strain rate equal to $10^{-5}\,s^{-1}$. Observations by X ray computerized tomography (CT) and scanning electron microscope (surface porosity) of specimens tested in compression showed a dilating shear band at 30 MPa and compacting shear band at 50 MPa confining pressure. The spatial resolution of the X ray apparatus is 0.7 mm for the lateral directions of the specimen and 2 mm for the axial direction. In the X ray reconstructions (Figure 7), an initial heterogeneity of the rock is illustrated by a density difference in the upper and lower half of the specimens. In the more porous half of the specimens (the darker half), the dilating shear band initiated during the test

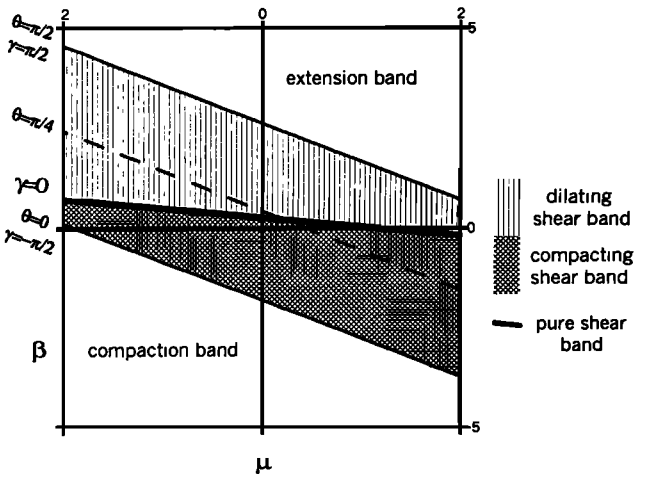

Figure 6. Distinction in the plane (μ, β) of the areas corresponding to the dilating and compacting shear bands and the extension and compaction bands, for an axisymmetric compression stress state ($N = 1/\sqrt{3}$) and $\nu = 0.2$.

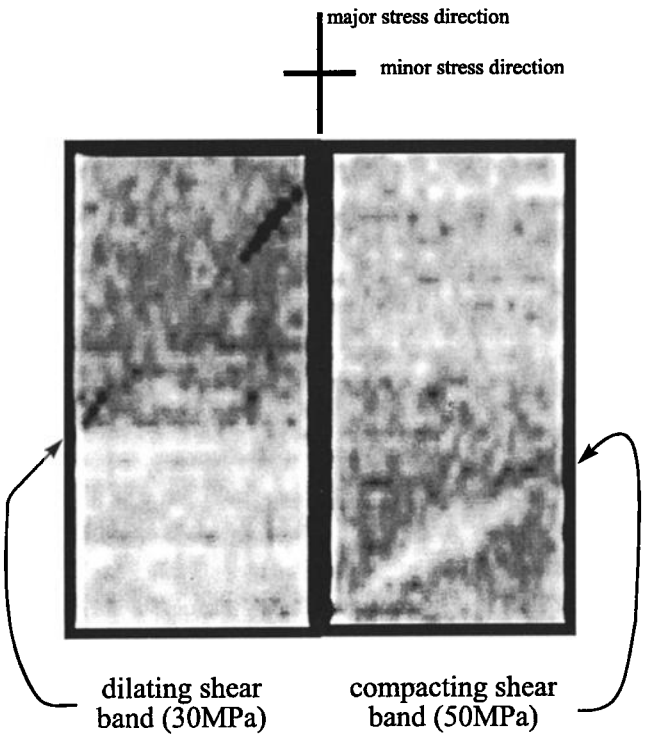

Figure 7. X ray CT reconstruction of specimens tested at 30 MPa (left, inclined dark band, dilating shear band) and 50 MPa (right, inclined light band, compacting shear band) confining pressure in triaxial compression test. Heterogeneity of the specimens (one half part is denser than the other part) already existed before the test.

is darker and the compacting shear band is lighter than outside the band.

Compressive stress and strain are assumed to be positive in this section. The elastic Poisson coefficient ν and the Young modulus are determined at the beginning of the axial loading when the stress-strain curves are quasi-linear. The friction coefficient μ is the slope of the theoretical yield surface in the Mises equivalent stress versus mean stress plane. Near the ultimate loading (i.e., near the onset of localization) this yield surface is assumed to be closed to the failure envelope determined from tests at several confining pressures [*Olsson*, 1999]. The Mohr envelope at failure (stress peak) in the shear stress versus normal stress plane (Figure 8) shows a strong nonlinearity, with a positive slope at low confining pressure and a negative slope at high confining pressure, and μ is approximated here as the local slope of the Mohr envelope multiplied by $2/\sqrt{3}$. For extension tests, the choice of μ is problematic and is arbitrarily taken to be the same as the value of μ determined from the uniaxial compression tests. Note that when the slope of the yield surface μ is negative, μ should not have the meaning of an internal friction coefficient. In this case, the negative value of μ occurs due to a decrease of shear strength as a result of grain crushing, which itself is due to high mean pressure.

During the experiments, the three axial and four lateral transducers enable detection of the loss of homogeneity of the strain field inside the specimen, which is associated with strain localization. Details of the strain measurements are given in *Bésuelle and Desrues* [2001]. The onset of localization was systematically observed before the stress peak. From these results, the parameter β associated with the plastic part of the RR formulation is determined at the onset of localization by the relation $\beta = -\sqrt{3}/2(\dot{\varepsilon}_a^p + 2\dot{\varepsilon}_l^p)/(\dot{\varepsilon}_a^p - \dot{\varepsilon}_l^p) \times \text{sign}\,(\sigma_a - \sigma_l)$, where $\dot{\varepsilon}_a^p$ and $\dot{\varepsilon}_l^p$ are the plastic axial and lateral strain rate and σ_a and σ_l are the axial and lateral stress (plastic strain is computed as the total strain minus the elastic strain determined from the elastic parameters). The hardening modulus h at the onset of localization is computed from the slope of the axial stress versus axial strain curves (see Figure 2b). The experimental parameters μ, β, ν, h, and θ, and the state of strain within the deformation bands are summarized in Table 1 for compression and extension tests conducted at confining pressures of 0 to 60 MPa.

The predicted values of θ_c, γ, and h_c are computed from the experimental data μ, β, and ν with (12), (21), and (13)-(14). The failure modes observed experimentally were differentiated by direct observation and CT imaging and compared with theoretical predictions: axial splitting (AS) is associated with a theoretical pure extension band (PE), the compacting shear bands (CB) predicted theoretically are associated with compacting shear bands observed inside the specimen, and theoretical dilating shear bands (DB) correspond to the experimental dilating shear bands. The volumetric strain inside the band of localization in extension tests has not been studied in specimens. At a confining pressure of 30-40 MPa the bands are parallel to the maximum principal stress direction. This observation suggests that the bands are dilating with nominally zero shear strain. The theoretical model predicts dilating shear bands for extension tests if the absolute magnitude of μ is assumed to be the same as the observed in uniaxial compression tests. However, at 30 MPa confining pressure, a small increase of μ up to 1.15 predicts a pure extension band, perpendicular to the least compressive stress direction as observed on the specimen. The angles between the band and the greatest compressive principal stress predicted for compression tests are

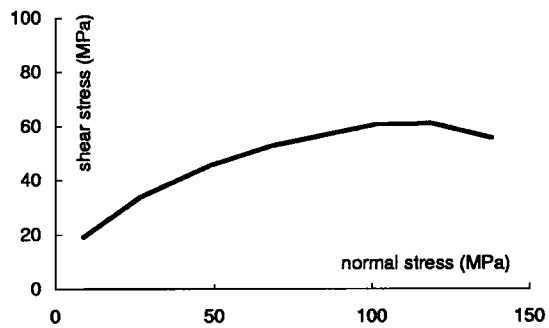

Figure 8. Failure surface of the sandstone in the Mohr plane.

Table 1. Experimental and Predicted Results in Axisymmetric Compression (C) and Extension (E) Tests for Several Confining Pressures from 0 to 60 MPa

	Experimental						Predicted		
Test	μ	θ, deg	β	ν	h/G	Mechanism[a]	Mechanism[a] (γ)	θ_c, deg	h_c/G
C: 0.5 MPa	0.97	90	1.55	0.4	~ 0.76	AS	PE (90°)	90	-1.37
C: 10 MPa	0.78	54	0.94	0.29	~ 0.03	DB	DB (66°)	67	-0.85
C: 20 MPa	0.56	50	0.73	0.21	~ -0.01	DB	DB (45°)	57	-0.61
C: 30 MPa	0.38	48	0.47	0.26	~ 0.04	DB	DB (27°)	52	-0.46
C: 40 MPa	0.20	47	0.26	0.26	~ 0.31	DB	DB (6°)	47	-0.33
C: 50 MPa	0.2 to	40	0.1	0.21	~ 0.78	CB	CB (-10°)	43	-0.27
	-0.1	...	...	...	...	...	CB (-16°)	39	-0.19
C: 60 MPa	-0.38	37	0	0.25	~ 1.47	CB	CB (-28°)	35	-0.10
E: 30 MPa	0.97	90	0.59	0.34	~ 0	PE	DB (75°)	78	0.03
	1.15	...	...	...	...	...	PE (90°)	90	0.07
E: 40 MPa	0.97	90[b]	0.4	0.33	~ 0	PE	DB (65°)	72	0.06
	1.15	...	...	...	...	...	DB (70°)	77	0 12
E: 50 MPa	0.97	71	0.43	0.37	~ 0	DB	DB (65°)	73	0.06
E: 60 MPa	0.97	69	0.37	0.4	~ 0	DB	DB (62°)	71	0.08

[a] Mechanisms of localization are: AS, axial splitting; PE pure extension band; DB, dilating shear band; CB, compacting shear band.
[b] Surfaces of failure in extension tests at low confining pressure (<40 MPa) were particularly influenced by a special shape of the specimen and are suspected to not be perfectly representative [*Bésuelle et al.*, 2000].

well in accordance with the measured angles. A maximum difference of 10° is observed at 10 MPa confining pressure, and values smaller than 45° are observed at high confining pressure. Similar results were reported by *Olsson* [1999]. The comparison of the experimental results (band angles and volumetric behavior inside the bands) and theoretical results suggests that the constitutive parameters associated with the homogeneous behavior before localization can be used to predict nature and orientation, and conditions necessary for the initiation of deformation bands.

4. Discussion

The above analysis for the strain mechanism of shear band formation predicts conditions for a reduction of the porosity inside a band. Small positive values of the dilatancy coefficient β and negative or small positive values of the friction coefficient μ are sufficient to explain such a behavior. Experimental results show that these conditions can be met when the mean pressure increases because both friction and dilatancy coefficients become small or negative. Such results enable a better understanding of the transition between localized deformation and cataclastic flow [*Bésuelle*, 2001]. This could be important during deformation of porous rocks in the crust.

From a micromechanical point of view, dilation within bands would occur when deformation is dominated by intergranular and intragranular microcracks. By contrast, compacting bands would arise when processes such as grain boundary sliding, grain rotation or grain crushing dominate.

The conditions for compacting shear bands are easier to reproduce in laboratory tests than conditions for pure compaction bands (pure normal strain), which require very low or negative values of the dilatancy coefficient and very high confining pressures. This latter strain type can be viewed as an endmember case of the compacting shear band, where the shear strain component becomes infinitesimal. These theoretical results enable interpretation of geological observations of bands with a low porosity in comparison with the porosity outside the band. Such analyses can be used to estimate the field stress conditions at the onset of localization by estimating the ratio between the shear and volumic strain inside the band. However, field observation of bands should be carefully considered because bands have generally sustained a large postlocalization history. *Antonellini et al.* [1994] have observed compacting shear bands in a porous sandstone. *Mollema and Antonellini* [1996] have observed bands with a reduction of porosity but no shear displacement, which may correspond to pure compaction bands.

The results presented here suggest that compacting shear bands can also exist in axisymmetric extension tests, as suggested from experimental considerations [*Bésuelle et al.*, 2000; *Zhu et al.*, 1997]. In this case, shear bands are oriented approximately parallel to the least principal stress direction. A high confining pressure should be necessary to produce them. By contrast, axial splitting characterized by cracks opening parallel to the compressive stress in uniaxial tests could be considered as extension bands.

The analysis of strain inside the band at the onset of localization shows values of μ ranging from about

-2.5 to 2.5, outside of which the continuity of the strain mechanism with respect to μ and β is not ensured. One could have a complete change of strain type inside the band for a small change in the constitutive parameter. This is a limit to the formulation of Rudnicki and Rice which has to be considered to model the mechanical behavior of rocks, although these theoretical restrictions on μ seem physically improbable.

The hardening modulus h is predicted to be negative in axisymmetric compression tests for the range of μ and β used, which means that localization should theoretically occur during strain softening. However, experimental data showed that localization occurs during strain hardening. This problem was discussed by RR, who considered as suspect the predicted onset of localization for the axisymmetric compression. A resolution of this problem depends on the mathematical formulation of the constitutive relations. Other laws predict localization in the hardening regime for axisymmetric stress condition [e.g., *Desrues and Chambon*, 1989].

5. Conclusions

Porous rocks have a specific behavior in that their yield surface is strongly nonlinear (i.e., the yield surface has a positive pressure dependence for low mean stress and a negative pressure dependence for high mean stress). This behavior is associated with the existence of dilating shear bands at low mean stress or even pure extension bands at very low stress (axial splitting), compacting shear bands at higher mean stress, and pure compaction bands at very high stress. This evolution from pure extension bands to pure compaction bands is continuous via shear bands. The latter are dilating at low stress and gradually become compacting with increasing mean stress, until they are purely compacting bands at high mean stress. The more compacting a band is, the higher the angle is between the band (the heavy line) and the major compressive stress direction, varying from 0 for pure extension band to $\pi/2$ for pure compaction band.

The angle between the shear bands and the principal stress directions depends on: the friction coefficient μ, the dilatancy factor β, Poisson's coefficient ν, and the stress state (i.e., N). For associated models ($\beta = \mu$), shear bands that have an angle with respect to the greatest principal stress direction that is lower than $\pi/4$ are dilating, while they are compacting if the angle is greater than $\pi/4$. For rocks that have a nonassociated behavior ($\beta \neq \mu$), the transition between dilating and compacting shear bands corresponds approximately to $\pi/4$.

The phenomenon of localized porosity reduction has important consequences for field applications, notably for transport of fluids. As was suggested for a pure compaction band [*Issen and Rudnicki*, 2000], compacting shear band can locally reduce the permeability and act as permeability barriers with preferential orientations, which may reduce (inducing a strong anisotropy) the global permeability of a geological structure.

Acknowledgments. I would like to thank Y. Guéguen and G. Simpson for their helpful discussions.

References

Antonellini, M. A., A. Aydin, and D. D. Pollard, Microstructure of deformation bands in porous sandstones at Arches National Park, Utah, *J. Struct. Geol., 16,* 941-959, 1994.

Bésuelle, P., Déformation et rupture dans les roches tendres et les sols indurés : Comportement homogène et localisation, Ph.D. thesis, 370 pp., Univ. of Grenoble, Grenoble, France, 1999.

Bésuelle, P., Evolution of strain localisation with stress in a sandstone: Brittle and semi-brittle regimes, *Phys. Chem. Earth, 26,* 101-106, 2001.

Bésuelle, P., and J. Desrues, An internal instrumentation for axial and radial strain measurements in triaxial tests, *Geotech. Test. J., 24,* 193-199, 2001.

Bésuelle, P., J. Desrues, and S. Raynaud, Experimental characterisation of the localisation phenomenon inside a Vosges sandstone in a triaxial cell, *Int. J. Rock Mech. Min. Sci., 37,* 1223-1237, 2000.

Desrues, J., and R. Chambon, Shear band analysis for granular materials: The question of incremental non-linearity, *Ing. Arch., 59,* 187-196, 1989.

Hicher, P.Y., and H. Wahyudi, Microstructural analysis of strain localisation in clay, *Comput. Geotech., 16,* 205-222, 1994.

Issen, K. A., and J. W. Rudnicki, Conditions for compaction bands in porous rock, *J. Geophys. Res., 105,* 21,529-21,536, 2000.

Mollema, P. N., and M. A. Antonellini, Compaction bands: A structural analog for anti-mode I cracks in aeolian sandstone, *Tectonophysics, 267,* 209-228, 1996.

Olsson, W. A., Theoretical and experimental investigation of compaction bands in porous rock, *J. Geophys. Res., 104,* 7219-7228, 1999.

Perrin, G., and J. B. Leblond, Rudnicki and Rice's analysis of strain localization revisited, *J. Appl. Mech., 4,* 842-846, 1993.

Rudnicki, J. W., A class of elastic-plastic constitutive laws for brittle rock, *J. Rheol., 28,* 759-778, 1984.

Rudnicki, J. W., and J. R. Rice, Conditions for the localization of deformation in pressure-sensitive dilatant materials, *J. Mech. Phys. Solids, 23,* 371- 394, 1975.

Tillard-Ngan, D., J. Desrues, and S. Raynaud, Strain localisation in beaucaire marl, in *Proceedings of Geotechnical Engineering of Hard Soils-Soft Rocks,* pp. 1679-1686, A.A. Balkema, Brookfield, Vt., 1993.

Wong, T.-F., C. David, and W. Zhu, The transition from brittle faulting to cataclastic flow in porous sandstone: Mechanical deformation, *J. Geophys. Res., 102,* 3009-3025, 1997.

Zhu, W., L. G. J. Montesi, and T.-F. Wong, Shear-enhanced compaction and permeability reduction: Triaxial extension tests on porous sandstone, *Mech. Mater., 25,* 199-214, 1997.

P. Bésuelle, Laboratoire de Géologie, Ecole Normale Supérieure, 24 rue Lhomond, 75231 Paris Cedex 05, France. (besuelle@geologie.ens.fr)

(Received March 31, 2000; revised November 21, 2000; accepted December 21, 2000.)